Bayesian three-dimensional reconstruction of toothed whale trajectories: Passive acoustics assisted with visual and tagging measurements

Christophe Laplanche[a)]
Université de Toulouse, INP, UPS, CNRS, EcoLab (Laboratoire Ecologie Fonctionnelle et Environnement), ENSAT, Avenue de l'Agrobiopole, 31326 Castanet Tolosan, France

The author describes and evaluates a Bayesian method to reconstruct three-dimensional toothed whale trajectories from a series of echolocation signals. Localization by using passive acoustic data (time of arrival of source signals at receptors) is assisted by using visual data (coordinates of the whale when diving and resurfacing) and tag information (movement statistics). The efficiency of the Bayesian method is compared to the standard minimum mean squared error statistical approach by comparing the reconstruction results of 48 simulated sperm whale (*Physeter macrocephalus*) trajectories. The use of the advanced Bayesian method reduces bias (standard deviation) with respect to the standard method up to a factor of 8.9 (13.6). The author provides open-source software which is functional with acoustic data which would be collected in the field from any three-dimensional receptor array design. This approach renews passive acoustics as a valuable tool to study the underwater behavior of toothed whales.

I. INTRODUCTION

Researchers have brought three main approaches into play to explore the behavior of toothed whales in the field: Visual, electronic tagging, and passive acoustics. Visual methods use photo-identification to differentiate individuals, map their surface movements, and catalogue their clustering preferences (Whitehead, 2003, pp. 206–285). Electronic tagging consists of attaching embedded systems on whales and record information on their subsequent behavior. Embedded systems can contain diverse receptors (acoustic, accelerometer, GPS, etc.) and provide as diverse information on whale behavior (Johnson *et al.*, 2009). Passive acoustics consists of recording whale sounds from dragged, hull-mounted, or bottom-mounted receptors and real-time or post-process signals (Houegnigan *et al.*, 2010; Miller and Dawson, 2009; Nielsen and Mohl, 2006). Toothed whales profusely use sound for communication and echolocation. All toothed whale species probe their underwater environment by emitting a series of transient, directive, high level clicks (Madsen and Wahlberg, 2007). Passive acoustic outcomes go beyond inference on whale acoustic behavior (Teloni *et al.*, 2008). Passive acoustics also leads to: Source detection in ambient noise (Sanchez–Garcia *et al.*, 2010), separation of multiple phonating individuals (Baggenstoss, 2011; Caudal and Glotin, 2008), localization (Cranch *et al.*, 2004; Hayes and Mellinger, 2000; Wahlberg *et al.*, 2001), inference on whale morphometry (Growcott *et al.*, 2011), and information on swim orientation during predation (Laplanche *et al.*, 2005, 2006; Nosal and Frazer, 2007). Each of the three latter approaches has pros and cons, by providing distinct pieces of information, with various equipment budget and time cost, and with different degrees of contact with whales. Whatsoever, all three approaches share a common feature: The need to localize the whale as a fundamental step in studying its behavior.

Passive acoustic localization is achieved by triangulating source signals on a synchronized array of receptors. Various designs of receptors have been operated to study the behavior of toothed whales: One-dimensional (Thode *et al.*, 2002), two-dimensional (Thode, 2004), or three-dimensional arrays (Cranch *et al.*, 2004; Hayes and Mellinger, 2000; Wahlberg *et al.*, 2001). Since times of emission of whale signals are unknown, triangulation is not achieved directly by using times of arrival (TOA) at receptors, but by using times of arrival differences (TOADs) at pairs of receptors. TOADs are later processed with statistical software to compute location estimates. One popular option is to derive a whale trajectory from minimum mean squared error (MMSE) estimates. The drawback of the latter approach is a high sensitivity to measurement errors resulting in broad inaccuracy (bias) and uncertainty (variance) on the estimate (Spiesberger, 2001; Wahlberg *et al.*, 2001). Bias and variance can be as large as to make localization results unhelpful.

The author presents an advanced statistical method of processing TOAD data which aim is to compute localization results of enhanced quality, that is to say of lower bias and variance than the standard method. The essence of the advanced method is to refine the processing of the acoustic data and to use nonacoustic data. Refined processing of the acoustic data will be achieved by reconstructing a whale trajectory while, and not afterwards, processing acoustic data. The interest of using nonacoustic data is to further improve the localization

[a)]Author to whom correspondence should be addressed. Electronic mail: laplanche@gmail.com

procedure (Davis and Pitre, 1995; Laplanche, 2007; Tiemann *et al.*, 2006). The complexity of the statistical model (high number of unknowns, non-linearities, heterogeneous sources of data) prevents the use of standard statistical tools but Bayesian modeling (Congdon, 2003, pp. 1–457). Bayesian modeling has already proven to be an efficient framework to address advanced issues in passive acoustic localization (Dosso and Wilmut, 2011; Spiesberger, 2005; Tollefsen and Dosso, 2010). The essence of Bayesian modeling is to (i) express (known) measured variables as functions of (unknown) latent variables, (ii) assign a prior distribution to the latent variables, (iii) calculate a mathematical expression of the posterior distribution of the latent variables, and (iv) use numerical methods to compute posterior estimates of the latent variables. The mathematical expression of the posterior distribution as well as the computation of posterior estimates are complex with complex models, making Bayesian modeling difficult to apply for researchers who are not familiar with computer programming and Bayesian statistics. Recent user-friendly Bayesian modeling tools, however, such as BUGS (Bayesian inference Using Gibbs Sampling), automatically calculate a mathematical expression and simulate the posterior [steps (iii) to (iv)], leaving only model formulation to users [steps (i) to (ii)], making Bayesian modeling more accessible (Ntzoufras, 2009, pp. 83–150).

The author first presents the standard localization procedure. This method is reformulated into a Bayesian context, before being extended, to get up to the full Bayesian localization method. The efficiency of both methods is compared by using simulated data, with the sperm whale (*Physeter marcocephalus*) as an example. The full Bayesian localization method could be of interest to study other toothed whale species, which is discussed.

II. MATERIALS AND METHODS

A. The standard statistical model

Sperm whales routinely undertake several hundred meters deep, 30 to 60-min dives (Whitehead, 2003, pp. 78–84, 156–168) interrupted by 10-min breathing breaks at the sea surface (Watwood *et al.*, 2006). Sperm whales are clearly visible and identifiable when breathing. Let us consider the full dive of some sperm whales, diving at time t_{dive} and resurfacing at time t_{resurf}. Sperm whale underwater acoustic activity is recorded on a synchronized array of receptors; let R be the number of acoustic receptors and $r \in \{1, \ldots, R\}$ be an index over receptors. Sperm whales emit several thousands of clicks through their dive; let us consider only a subsample of these clicks, where K denotes the number of processed clicks and $k \in \{1, \ldots, K\}$ an index over clicks. Let t_k be the time of emission of click k, $t_{\text{dive}} < t_1 < \cdots < t_K < t_{\text{resurf}}$. Let $(x^h_{r,k}, y^h_{r,k}, z^h_{r,k})$ be the Cartesian coordinates of receptor r at time t_k. The measured value of TOA of click k on receptor $r (r \in \{1, \ldots, R\})$ is denoted $\text{TOA}_{r,k}$. By using the first receptor as a baseline, the measured value of TOAD of click k on receptor r $(r \in \{2, \ldots, R\})$ is denoted $\text{TOAD}_{r,k}$.

Let $M_k = (x_k, y_k, z_k)$ be the Cartesian coordinates of the whale at time t_k. By using the spherical propagation model, c is the sound speed, the predicted value of TOA of click k on receptor $r (r \in \{1, \ldots, R\})$ is

$$\overline{\text{TOA}}_{r,k} = t_k + \frac{1}{c}\sqrt{(x_k - x^h_{r,k})^2 + (y_k - y^h_{r,k})^2 + (z_k - z^h_{r,k})^2}. \tag{1}$$

And by using the first receptor as baseline, the predicted value of TOAD of click k on receptor $r (r \in \{2, \ldots, R\})$ is

$$\overline{\text{TOAD}}_{r,k} = \overline{\text{TOA}}_{r,k} - \overline{\text{TOA}}_{1,k}. \tag{2}$$

The MMSE point estimate of $(M_1, \ldots, M_K)$ minimizes the quadratic sum of the residuals $S^2 = \sum_{k=1}^{K} S_k^2$ where

$$S_k^2 = \sum_{r=2}^{R} (\text{TOAD}_{r,k} - \overline{\text{TOAD}}_{r,k})^2. \tag{3}$$

The minimum of S^2 is actually reached by minimizing each S_k^2 separately. The implications of the latter assertion are first that the $3K$-dimension optimization problem (minimizing S^2) can be handled without difficulty by partitioning it into K three-dimension optimization problems (minimizing S_k^2 for all k) and using a standard optimization method. Second, acoustic data at time t_k is only used to compute an estimate of the location of the whale at the exact same time. In view of whale inertia, measured values $\text{TOAD}_{r,k}$ actually contain information on the location of the whale *around* time t_k. The advanced Bayesian model which will be presented later will process acoustic data in this perspective. The advanced model is an extension of a Bayesian reformulation of the standard model, which is presented below.

B. Bayesian formulation of the standard model

MMSE estimates are approximately equal to expectation *a posteriori* (EAP) estimates by using a Bayesian statistical model with independent, normally distributed residual errors of equal variance and vague priors (Appendix A). Such a statistical model is defined by Eqs. (1) and (2) plus following Eqs. (4) to (6). Let Normal(μ, σ^2) denote some Normal variate of expectation μ and variance σ^2 and Gamma(α, β) some Gamma variate of shape α and scale β. Measured TOAD values are modeled as independent, normally distributed variates of expectation predicted TOAD values and of variance σ_τ^2

$$\text{TOAD}_{r,k} \sim \text{Normal}(\overline{\text{TOAD}}_{r,k}, \sigma_\tau^2), \tag{4}$$

where σ_τ^2 is the variance of the TOAD residual error. Vague priors are assigned to the Cartesian coordinates of the whale

$$x_k,\ y_k,\ z_k \ \sim\ \text{Normal}(0, 10^8), \tag{5}$$

and to the variance of the residual error

$$1/\sigma_\tau^2 \sim \text{Gamma}(10^{-3}, 10^{-3}). \tag{6}$$

See Appendix A for a mathematical expression of the posterior of this model. Relationships between model variables

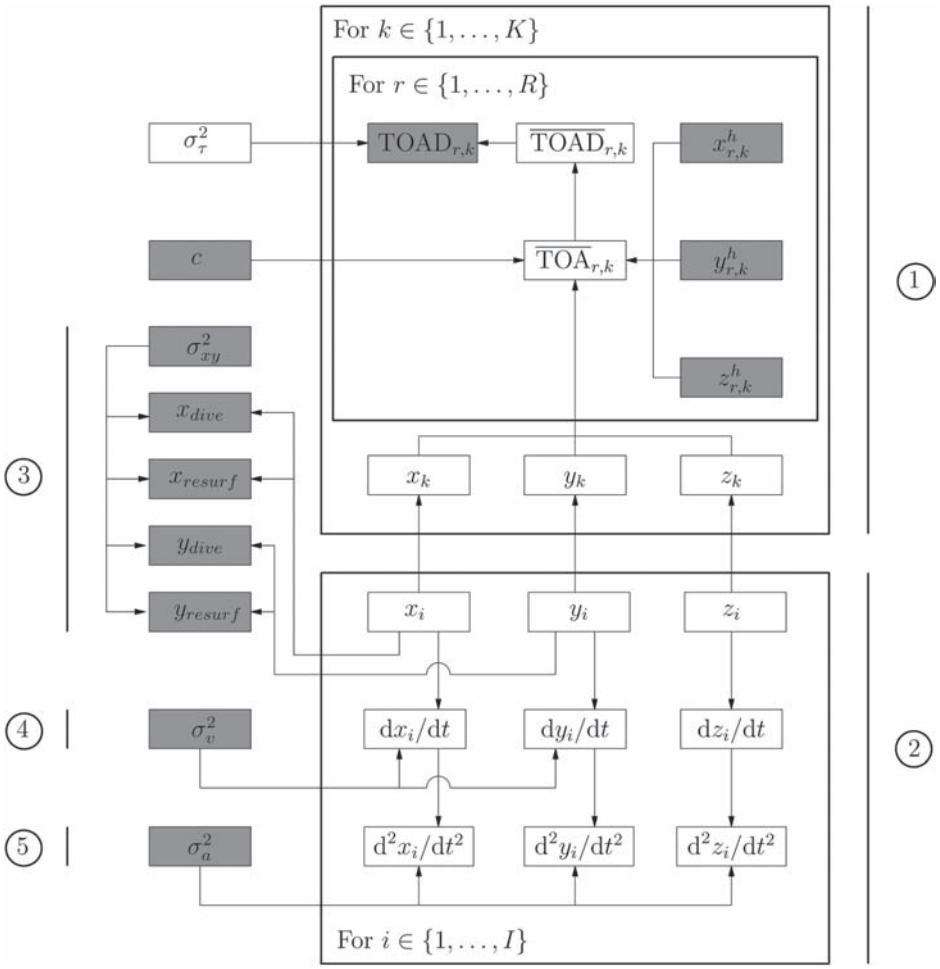

FIG. 1. DAG of the full model. Frames indicate levels: Receptor ($r \in \{1,\ldots,R\}$), click ($k \in \{1,\ldots,K\}$), and trajectory segment ($i \in \{0,\ldots,I\}$). White rectangles: Latent variables; filled rectangles: observed variables; circles: model components. The standard model reduces to model component 1. The standard model connects whale coordinates (x_k, y_k, z_k), receptor coordinates $(x^h_{r,k}, y^h_{r,k}, z^h_{r,k})$, and acoustic data $\mathrm{TOAD}_{r,k}$ to each other. The full model is an extension of the standard model by adding a trajectory model (model component 2), visual data (component 3), speed statistics (component 4), and acceleration statistics (component 5).

are illustrated with a Directed Acyclic Graph (DAG, Fig. 1). The full model is an extension of the standard model by including a trajectory model, visual data, speed statistics, and acceleration statistics.

C. Whale trajectory

The underwater movement of the whale is modeled as a continuous series of segments of uniform linear motion and of equal duration (Fig. 2). Let I be the number of segments, $\Delta_I = (t_{\mathrm{resurf}} - t_{\mathrm{dive}})/I$ be the duration of the segments, and $t_i = t_{\mathrm{dive}} + i\Delta_I (i \in \{0,....,I\})$. Let $M_i = (x_i, y_i, z_i)$ be the location of the whale at time t_i, and $[M_i M_{i+1}]$ be the segments which make up the modeled trajectory. With this model, the location of the whale at time t_k is $M_k = (x_k, y_k, z_k)$ with

$$x_k = x_{i_k} + \frac{x_{i_k+1} - x_{i_k}}{t_{i_k+1} - t_{i_k}}(t_k - t_{i_k}), \tag{7}$$

and similar formulas for y_k and z_k, where $i_k \in \{0,\ldots,I-1\}$ is the index of the trajectory segment where the whale is located at time t_k. Predicted TOAD at time t_k is still provided by Eqs. (1) and (2) and the relationship between measured and predicted TOAD values is still given by Eq. (4). Relationships between model variables are illustrated in Fig. 1. Free parameters of the model are the Cartesian coordinates (x_i, y_i, z_i) as well as the variance of the residual error σ_τ^2. A vague prior is assigned to the Cartesian coordinates of the whale

$$x_i, y_i, z_i \sim \mathrm{Normal}(0, 10^8), \tag{8}$$

and a vague prior is assigned to the variance of the residual error [Eq. (6)].

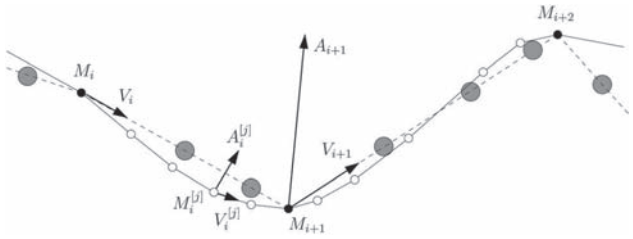

FIG. 2. The whale movement is modeled as a series of segments of uniform linear motion. The trajectory model is represented at two time steps, infinitesimal (full line, white and black dots) and at a larger time step (dashed line, black dots only). At an infinitesimal time step, $M_i^{[j]} = (x_i^{[j]}, y_i^{[j]}, z_i^{[j]})$, $V_i^{[j]} = (\mathrm{d}x_i^{[j]}/\mathrm{d}t, \mathrm{d}y_i^{[j]}/\mathrm{d}t, \mathrm{d}z_i^{[j]}/\mathrm{d}t)$ and $A_i^{[j]} = (\mathrm{d}^2x_i^{[j]}/\mathrm{d}t^2, \mathrm{d}^2y_i^{[j]}/\mathrm{d}t^2, \mathrm{d}^2z_i^{[j]}/\mathrm{d}t^2)$ are the location, the speed, and the acceleration of the whale at time $t_i^{[j]}$. At a larger time step, $M_i = (x_i, y_i, z_i)$ is the location of the whale at time t_i, $V_i = (\mathrm{d}x_i/\mathrm{d}t, \mathrm{d}y_i/\mathrm{d}t, \mathrm{d}z_i/\mathrm{d}t)$ is the average speed of the whale on segment i, and $A_{i+1} = (\mathrm{d}^2x_{i+1}/\mathrm{d}t^2, \mathrm{d}^2y_{i+1}/\mathrm{d}t^2, \mathrm{d}^2z_{i+1}/\mathrm{d}t^2)$ is the acceleration of the whale when passing from segment i to segment $i+1$. The modeled location of the whale at click time t_k by using the trajectory model with a non-infinitesimal time step are also illustrated (M_k, gray circles). Mathematical relationships between $M_i, V_i, A_i, M_i^{[j]}, V_i^{[j]}, A_i^{[j]}$ are provided in Appendix C. The expression of M_k is given in the text.

D. Visual data

Sperm whales are clearly visible and identifiable when breathing (Whitehead, 2003, pp. 206–285). Let $(x_{\text{dive}}, y_{\text{dive}}, 0)$ and $(x_{\text{resurf}}, y_{\text{resurf}}, 0)$ be the measured values of the Cartesian coordinates of the whale at time t_{dive} and t_{resurf}. Deviations between predicted and measured values are tolerated and are modeled as independent normally distributed errors of variance σ_{xy}^2

$$x_{\text{dive}} \sim \text{Normal}(x_0, \sigma_{xy}^2), \tag{9}$$

and similar formulas for y_{dive}, x_{resurf}, and y_{resurf}. The predicted depths when diving and resurfacing are forced to be exactly equal to zero, $z_0 = 0$ and $z_I = 0$.

E. Speed statistics

Sperm whales initiate and end dives by being silent and by swimming substantially vertically (Watwood *et al.*, 2006). Let $V_i = (M_{i+1} - M_i)/\Delta_I$ be the average speed of the whale on segment i (Fig. 2). The Cartesian coordinates of V_i are denoted $(\mathrm{d}x_i/\mathrm{d}t, \mathrm{d}y_i/\mathrm{d}t, \mathrm{d}z_i/\mathrm{d}t)$ with $dx_i/dt = (x_{i+1} - x_i)/\Delta_I$ (and similar formulas for $\mathrm{d}y_i/\mathrm{d}t$ and $\mathrm{d}z_i/\mathrm{d}t$, $i \in \{0, \ldots, I-1\}$). Let $\{0, \ldots, i_{\text{start}} - 1\}$ and $\{i_{\text{stop}} - 1, \ldots, I - 1\}$ be the index of segments while the whale is silent at the beginning and at the end of the dive, respectively. The horizontal speed of the whale for $i \in \{0, \ldots, i_{\text{start}} - 1\} \cup \{i_{\text{stop}} - 1, \ldots, I - 1\}$ is modeled as independent, normally distributed variates of expectation 0 and of variance σ_v^2/Δ_I

$$\frac{\mathrm{d}xi}{\mathrm{d}t}, \frac{\mathrm{d}yi}{\mathrm{d}t} \sim \text{Normal}(0, \sigma_v^2/\Delta_I), \tag{10}$$

where σ_v^2 is the variance of the horizontal speed of the whale which would be measured by using a speed recording device at a 1 s time step (see Appendix C).

F. Acceleration statistics

Sperm whale acceleration is limited due to hydrodynamic drag (Miller *et al.*, 2004). Let $A_i = (V_i - V_{i-1})/\Delta_I$ be the acceleration of the whale when passing from segment $i-1$ to segment i (Fig. 2). The Cartesian coordinates of A_i are noted $(\mathrm{d}^2x_i/\mathrm{d}t^2, \mathrm{d}^2y_i/\mathrm{d}t^2, \mathrm{d}^2z_i/\mathrm{d}t^2)$ with $\mathrm{d}^2x_i/\mathrm{d}t^2 = (\mathrm{d}x_i/\mathrm{d}t - \mathrm{d}x_{i-1}/\mathrm{d}t)/\Delta_I$ (and similar formulas for $\mathrm{d}^2y_i/\mathrm{d}t^2$ and $\mathrm{d}^2z_i/\mathrm{d}t^2$, $i \in \{1, \ldots, I-1\}$). The acceleration of the whale is modeled as independent, normally distributed variates of expectation 0 and of variance σ_a^2/Δ_I

$$\frac{\mathrm{d}^2x_i}{\mathrm{d}t^2}, \frac{\mathrm{d}^2y_i}{\mathrm{d}t^2}, \frac{\mathrm{d}^2z_i}{\mathrm{d}t^2} \sim \text{Normal}(0, \sigma_a^2/\Delta_I), \tag{11}$$

where σ_a^2 is the variance of the acceleration of the whale which would be measured by using an acceleration recording device at a 1 s time step (see Appendix C).

G. Dataset

The author compares the efficiency of the standard and the full Bayesian methods with a simulated dataset. The interest of using a simulated dataset is to have at one's disposal true values, and compare them to estimated values. The author considers 48 simulated whale trajectories. An example of a trajectory is illustrated in Figs. 3 and 4. The whale dives at some arbitrary point ($x_{\text{dive}} = 500$, $y_{\text{dive}} = 0$ m) at $t_{\text{dive}} = 0$, starts clicking at $t_{\text{start}} = 2$ min, stops clicking at $t_{\text{stop}} = 30$ min, and resurfaces at $t_{\text{resurf}} = 40$ min. Trajectories are randomly generated in accordance with the autoregressive model of Appendix C with $\sigma_v = 0.1$ m/s, $\sigma_a = 0.05$ m/s^2, and $\Delta_t = 1$ s.

Sperm whale clicks are recorded on three hydrophones. Hydrophones are initially located at (0, 0, −30) m, (−200, 0, −40) m, and (0, 200, −50) m. All hydrophones drift Northeast at 0.1 m/s. Both direct and surface-reflected source signals are assumed to be detected on the receptors, leading to a virtual array of six hydrophones (Skarsoulis and Kalogerakis, 2005). The author investigates the consequences of the variations of the quantity and the quality of the acoustic dataset by considering two click rates as well as two noise levels. Two series of predicted TOAD values are computed for each trajectory, at a slow rate (1 click every $\Delta_K = 30$ s, $K = 57$) and at a high rate (1 click every $\Delta_K = 5$ s, $K = 337$). A white Gaussian noise of standard deviation $\sigma_\tau = 0.1$ ms or $\sigma_\tau = 1$ ms is added to the predicted TOAD values, leading to 4 acoustical datasets for each trajectory. Furthermore, two levels of trajectory resolution are compared by using the full Bayesian model: Low-resolution trajectories, with $\Delta_I = 60$ s segments ($I = 40$), and smoother trajectories, with $\Delta_I = 10$ s segments ($I = 240$). Acoustic data at a slow click rate are processed with the standard model and with the full model at a low-resolution and acoustic data at a high click rate are processed with the standard model and with the full model at a high-resolution. As a summary, a total of 384 simulations are carried out: 48 trajectories, 2 noise levels, 2 click rates, and 2 models.

H. Software

Models are implemented in BUGS language by using OpenBUGS, an open source version of WinBUGS (Ntzoufras, 2009, pp. 1–492). The creation of input files for BUGS, as well as the gathering of BUGS output files in order to compute trajectory statistics and display, is achieved with *R*. BUGS and *R* scripts are gathered within the open-source software SBPLAsH version 2.0 (http://modtox.myftp.org/software/sbplash). Users can provide input files and explore simulation results through SBPLAsH graphical user interface. SBPLAsH also creates Unix batch and portable batch system scripts to perform parallel BUGS computations on a UNIX desktop computer or a high performance computing (HPC) resource. See Appendix B for more computational details.

I. Model comparisons

Models are compared in terms of goodness-of-fit and complexity (Appendix B) as well as accuracy and uncertainty. The average absolute bias $\bar{\Delta}_x = \sum_{k=1}^{K} |x_k - \hat{x}_k|/K$ (with similar formulas for $\bar{\Delta}_y$ and $\bar{\Delta}_z$) is used as a proxy of model accuracy, where $\hat{x}_k$ denotes the estimate of x_k. The average standard deviation $\bar{\Sigma}_x = \sum_{k=1}^{K} \hat{\sigma}_{x,k}/K$(with similar

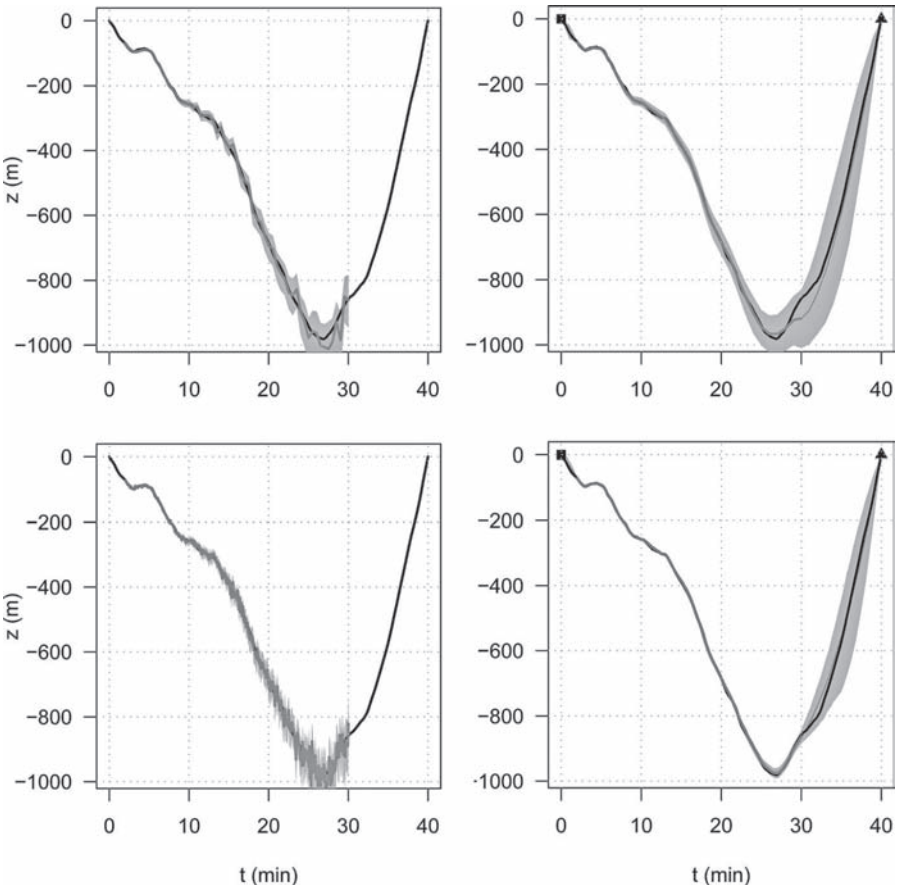

FIG. 3. Whale depth. True value (black line), point estimate (dark gray line), 95% interval estimates (light gray polygon), diving point (black square), and resurfacing point (black triangle). Acoustic data from 1 of the 48 whale trajectories at a low noise level ($\sigma_\tau = 0.1$ ms) is processed by using the standard model (left) or the full model (right) and by processing clicks at a slow rate (top, $\Delta_K = 30$ s) or high rate (bottom, $\Delta_K = 5$ s). Respective *xy*-coordinate values are illustrated in Fig. 4.

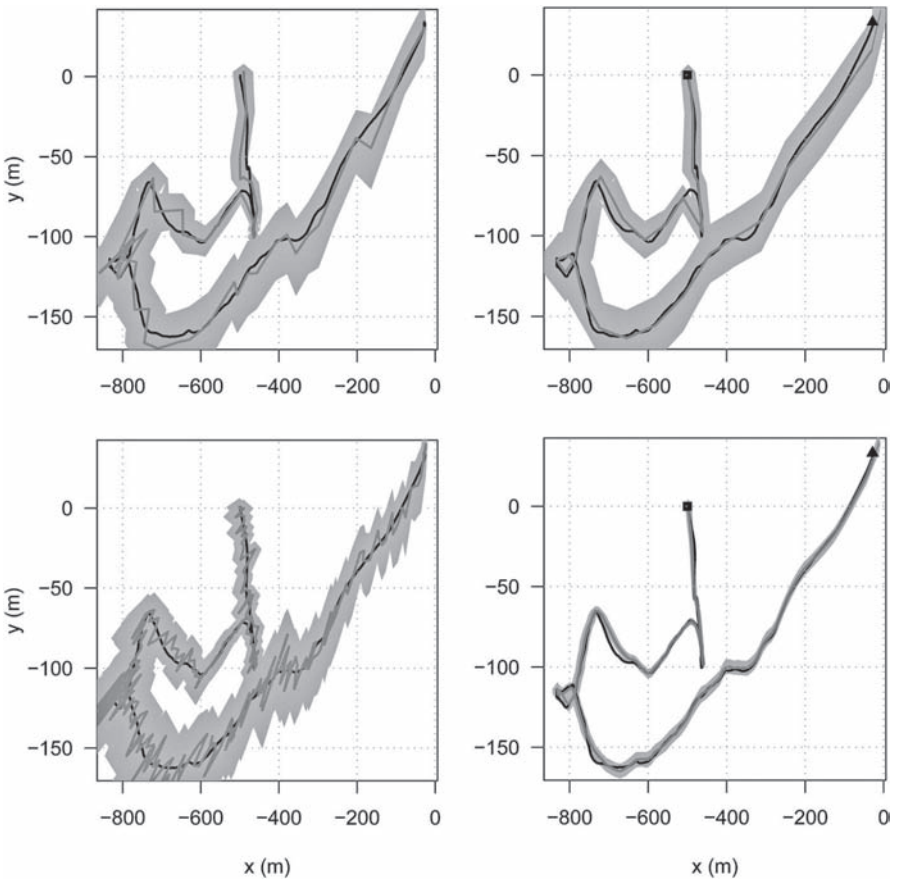

FIG. 4. Whale *xy* coordinates. See legend of Fig. 3.

formulas for $\bar{\Sigma}_y$ and $\bar{\Sigma}_z$) is used as a proxy of model uncertainty, where $\hat{\sigma}_{x,k}$ denotes the estimate of the standard deviation of the posterior of x_k.

III. RESULTS

Simulation results are illustrated in Figs. 3 and 4, with one of the 48 trajectories as an example, with acoustic data at a low noise level ($\sigma_\tau = 0.1$ ms). Simulation results for other combinations of trajectory, noise level, and click rate are provided as supplementary material. Accuracy and uncertainty for each of the eight combinations of noise level, click rate, and model are averaged over trajectories and are provided in Table I.

The results show, in each case, that the full model is more accurate and less uncertain than the standard model. At a low noise level and by processing one click every $\Delta_K = 30$ s, using the full model rather than the standard model reduces bias (standard deviation) by a factor 1.9 (2.2). Results of the standard model at a high noise level are unhelpful (bias: 156 m; standard deviation: 210 m). A standard deviation of 210 m corresponds to a 95% confidence interval which is approximately 880 m wide. At a high noise level and by processing one click every $\Delta_K = 30$ s, using the full model rather than the standard model reduces bias (standard deviation) by a factor 5.3 (5.7). The processing of a higher number of clicks does not improve localization results by using the standard model. Results are improved when using the full model. At a low noise level and by processing one click every $\Delta_K = 5$ s, using the full model rather than the standard model reduces bias (standard deviation) by a factor 4.2 (7.4). At a high noise level, bias (standard deviation) is reduced by a factor 8.9 (13.6) and reach an acceptable level (bias: 17.6 m; standard deviation: 15.5 m).

IV. DISCUSSION

Results show that processing TOAD data with the standard approach provides biased, uncertain outputs. Localization results range from inaccurate and uncertain (at a low noise level) to unhelpful (at a high noise level). The reasons for that are (1) to process acoustic signals independently of one another and (2) to discard additional, nonacoustic information which could be of interest in the localization procedure. The joint processing of acoustic data with a trajectory model, the consideration of visual measurements, and the use of prior knowledge on whale trajectory statistics has significantly enhanced localization results. Localization results by using the full model range from highly accurate at a low noise level (bias: 6.1 m; standard deviation: 4.5 m) to helpful at a high noise level (bias: 17.6 m; standard deviation: 15.5 m). OpenBUGS software offers a handy framework to operate Bayesian models, SBPLAsH software provides a user-friendly interface to operate the localization models, and both softwares are open-source. Consequently, the author encourages bioacousticians to use SBPLAsH and explore the capabilities of Bayesian methods to locate sound sources to a higher accuracy.

TABLE I. Bias ($\bar{\Delta}$) and standard deviation ($\bar{\Sigma}$) of the standard and the full models at two noise levels ($\sigma_\tau = 0.1$ ms and $\sigma_\tau = 1$ ms) and two click rates ($\Delta_K = 30$ and $\Delta_K = 5$ s). Bias and standard deviation are averaged over trajectories, clicks, and spatial dimensions. Ratios of averaged bias and standard deviations are also provided.

	σ_τ (ms)	0.1		1	
Model	Δ_K (s)	30	5	30	5
Standard	$\bar{\Delta}_s$(m)	28.5	25.6	155.8	156.1
	$\bar{\Sigma}_s$(m)	34.9	33.5	211.2	209.7
Full	$\bar{\Delta}_f$(m)	15.2	6.1	29.2	17.6
	$\bar{\Sigma}_f$(m)	16.1	4.5	37.2	15.5
$\frac{\text{standard}}{\text{full}}$	$\bar{\Delta}_s/\bar{\Delta}_f$(m)	×1.9	×4.2	×5.3	×8.9
	$\bar{\Sigma}_s/\bar{\Sigma}_f$(m)	×2.2	×7.4	×5.7	×13.6

The software do not require any update at all to run with a three-dimensional array design which would be different from the one which has been used as an example. The reason is that the number of receptors as well as the coordinates of the receptors are provided as inputs to the software. While SBPLAsH in its current version requires the coordinates of the receptors to be known, a minor update would be required for SBPLAsH to be operative with unknown receptor coordinates. Indeed, TOADs contain information on the locations of both the whale and the receptors. Spiesberger (2005) has already shown that it is possible to compute reliable estimates of source and receptor coordinates from TOAD data with a Bayesian model. The minor update to SBPLAsH would be to process receptor coordinates $(x^h_{r,k}, y^h_{r,k}, z^h_{r,k})$ as latent variables instead of measured variables. Receptor coordinates would be inferred from TOAD data for the same reasons as whale coordinates.

The method has been evaluated with simulated data. The parameters of the autoregressive trajectory model (σ^2_v and σ^2_a) need to be adjusted for the method to be operative in the field. Adjusted values could be computed for sperm whales by using past measurements from data loggers with accelerometers (Johnson *et al.*, 2009). The model could be recalibrated and used to locate species of genera *Hyperoodon*, *Mesoplodon*, or *Ziphius*, whose underwater behaviors are very close to a sperm whale's (Baird *et al.*, 2006; Hooker and Baird, 1999). The method could also be used to locate smaller toothed whales. In that case, the time resolution of the model (Δ_I and Δ_K) should also be updated. At last, with the same limitations as above, the method could be used to locate other echolocating marine mammals such as *Mirounga* species.

Users need to process raw acoustic recordings and compute TOADs before running SBPLAsH. For that purpose, users need to (1) detect clicks in ambient noise, (2) identify clicks across receptors, and (3) compute TOAs and TOADs. Several algorithms have been developed to detect transient whale signals in ambient noise (Yack *et al.*, 2010). The rate of emission of toothed whale clicks is highly variable during predation, which facilitates multi-path separation at a single receptor (Baggenstoss, 2011) or identification of source signals across receptors. TOAs and TOADs can be computed by using a cross-correlation or related method (Carter, 1987). Whereas the use of SBPLAsH at the current version

to reconstruct the trajectory of isolated toothed whales is an appealing perspective, the use of SBPLAsH is somewhat premature to localize groups of individuals. Separation of echolocation signals originating from groups of toothed whales is a difficult task indeed. The interest of coupling source separation and localization has already been demonstrated (Bahl *et al.*, 2004; Caudal and Glotin, 2008; Hirotsu *et al.*, 2008, 2010). To the authors' point of view, Bayesian modeling is a promising approach on this prospect, in view of the superiority of the approach to handle source separation (Rowe, 2002, pp. 169–206) and the capabilities of the approach to achieve localization. Bayesian modeling, by providing a flexible framework to statistically handle heterogeneous data, opens up new horizons for renewing passive acoustics as a valuable tool to study the behavior of toothed whales.

ACKNOWLEDGMENTS

This work was granted access to the HPC resources of CALMIP under the allocation 2012-P1113. The author is grateful to the anonymous referees for their valuable comments.

APPENDIX A: TOWARD A BAYESIAN EXPRESSION OF THE STANDARD MODEL

Let $\boldsymbol{M}=(M_1,\ldots,M_K)$ and $\mathbf{TOAD}=(\mathrm{TOAD}_{2,1},\ldots,\mathrm{TOAD}_{R,K})$. Under the assumption of independent, normally distributed residual errors of equal variance σ_τ^2, measured and predicted TOAD values are related by Eq. (4). In that case, the likelihood of the TOAD dataset is

$$p(\mathbf{TOAD}|\boldsymbol{M},\sigma_\tau^2)=\frac{1}{\sqrt{2\pi\sigma_\tau^{2^n}}}\exp(-S^2/2\sigma_\tau), \tag{A1}$$

where the maximum is reached by minimizing S^2. MMSE estimates are therefore equal to maximum likelihood (ML) estimates under the assumption of independent, normally distributed residual errors of equal variance. Moreover, ML estimates are equal to maximum *a posteriori* (MAP) estimates by choosing flat, uniformative priors. Indeed, by using Bayes' theorem, the prior $p(\boldsymbol{M},\sigma^2)$ and the posterior $p(\boldsymbol{M},\sigma^2|\mathbf{TOAD})$ of the model parameters are related as follows:

$$p(\boldsymbol{M},\sigma^2|\mathbf{TOAD})p(\mathbf{TOAD})=p(\mathbf{TOAD}|\boldsymbol{M},\sigma^2)p(\boldsymbol{M},\sigma^2). \tag{A2}$$

The posterior is proportional to the likelihood by using the flat prior $p(\boldsymbol{M},\sigma^2)=1$, and as a corollary, ML and MAP estimates are equal. Flat priors are not proper distributions, however, and low-informative (also known as vague) distributions should be used instead (Lambert *et al.*, 2005). A usual choice is to assign conjugate prior distributions with large variance. The whale coordinates are assigned a vague normal prior [Eq. (5)] and the residual variance is assigned a vague inverse-gamma prior [Eq. (6)]. By using vague priors, MAP and ML estimates are substantially equal. Finally, EAP estimates are more easily obtainable by using Monte Carlo Markov chain (MCMC) numerical methods than MAP estimates. EAP estimates are equal to MAP estimates for unimodal, symmetric posterior distributions. The latter property can easily be checked from MCMC simulations. As a conclusion, under the limitations provided above, EAP and MMSE estimates are substantially equal to each other, and the Bayesian expression of the standard model can be used to compute approximate MMSE estimates.

APPENDIX B: COMPUTATIONAL DETAILS

BUGS simulates posterior parameter samples by using a Markov chain Monte Carlo (MCMC) method (Ntzoufras, 2009). MCMC methods produce an ergodic chain of parameter samples which stationary distribution is their posterior (Robert and Casella, 2010, pp. 267–320). Consequences are three-fold: first, some time is required for the MCMC method to converge; second, some more time is required to have enough samples to provide relevant posterior statistics; and third, both latter assertions are true no matter which initial parameter value is chosen. An astute choice of initial value can, however, reduce time to convergence and as a result reduce overall computation time. Initial values were chosen as follows: Initial values of the standard model are $x_k=y_k=0$ and $z_k=-300\,\mathrm{m}$ ($k\in\{1,\ldots,K\}$), estimated values of the standard model at a low resolution (for a given trajectory and noise level) are used to initialize the full model at a low-resolution (for the same trajectory and noise level), and estimated values of the full model at a low-resolution are used to initialize the full model at a high-resolution. Convergence was unambiguous by inspection of the simulated MCMC samples. The total number of simulated samples for each run is provided in Table II, the first half was discarded for convergence purposes. Subsequent parameter samples are autocorrelated. Thinning (e.g., keep one sample every 1000) guided by the examination of the autocorrelation function of the parameter samples is a good option in order to produce a series of independent samples and correctly set the total number of MCMC iterations. Five hundred independent samples were saved for each run. As an illustration, 10^6 samples were simulated by using the standard model with $\sigma_\tau=0.1\,\mathrm{ms}$ and $\Delta_K=5\,\mathrm{s}$, the first 500 000 were discarded, 1 sample every 1000 was kept among the 500 000 next samples, in order to produce 500 independent samples. Simulation times are provided in Table II. Each simulation was run on a single core of a 2.8 Ghz quad-core Nehalem EX. Simulations were run on a HPC resource in order to process trajectory data on 48 cores.

TABLE II. Total number of iterations and computation times of the standard and full models at two noise levels ($\sigma_\tau=0.1\,\mathrm{ms}$ and $\sigma_\tau=1\,\mathrm{ms}$) and two click rates ($\Delta_K=30$ and $\Delta_K=5\,\mathrm{s}$).

	σ_τ (ms)	0.1		1	
Model	Δ_K (s)	30	5	30	5
Standard	iterations ($\times10^6$)	0.5	1	1	2
	time (h)	0.2	0.8	0.3	1.8
Full	iterations ($\times10^6$)	1	2	2	4
	time (h)	0.8	11.0	1.8	21.0

TABLE III. Goodness-of-fit ($\bar{D}$) and complexity (p_D) of the standard and full models at two noise levels ($\sigma_\tau = 0.1$ ms and $\sigma_\tau = 1$ ms) and two click rates ($\Delta_K = 30$ and $\Delta_K = 5$ s). Goodness-of-fit and complexity are averaged over trajectories.

	σ_τ (ms)	0.1		1	
Model	Δ_K (s)	30	5	30	5
Standard	$\bar{D}$	−321.7	−1961.5	943.2	5609.4
	p_D	169.9	962.1	130.2	768.4
Full	$\bar{D}$	182.2	−1892.8	990.0	5921.8
	p_D	123.3	719.8	121.9	718.3

The 500 independent samples of each run are used to compute point, interval, and standard deviation estimates of the model parameters. Reported point estimates are EAP estimates and reported interval estimates are 2.5% and 97.5% posterior marginal quantiles. Point and interval estimates of (x_k, y_k, z_k) [and (x_i, y_i, z_i) by using the full model] are used to compute whale trajectories (Figs. 3 and 4). Point and standard deviation estimates of (x_k, y_k, z_k) are used to compute model bias and variance (Table I). Posterior expectation of the deviance statistics (denoted $\bar{D}$) is used as an index of goodness-of-fit. The latter statistics are computed by calculating the likelihood with respect to the TOAD dataset [Eq. (A1)], before calculating the deviance (minus 2 times the log likelihood) and averaging over MCMC samples. Models can be compared in term of goodness-of-fit—the lower the deviance the better the fit—to the strict limitation that compared indexes are computed by using the exact same dataset. The four datasets which are simulated for each trajectory—two different noise levels and two different click rates—are distinct. Model complexity (denoted p_D) is computed as described by Spiegelhalter *et al.* (2002), which is a better representation of model complexity than a manual count of free parameters. Averaged values of goodness-of-fit and complexity are provided in Table III.

Baggenstoss, P. M. (**2011**). "Separation of sperm whale click-trains for multipath rejection," J. Acoust. Soc. Am. **129**(6), 3598–3609.

Bahl, R., Nakatani, T., Ura, T., and Sakata, M. (**2004**). "Automatic classification of diving sperm whales by analysis of click time delay using two hydrophones," in *Proceedings of the IEEE Oceans'04*, pp. 2316–2320.

Baird, R. W., Webster, D. L., McSweeney, D. J., Ligon, A. D., Schorr, G. S., and Barlow, J. (**2006**). "Diving behaviour of Cuvier's (*Ziphius cavirostris*) and Blainville's (*Mesoplodon densirostris*) beaked whales in Hawaii," Can. J. Zool. **84**(8), 1120–1128.

Carter, G. (**1987**). "Coherence and time-delay estimation," Proc. IEEE **75**, 236–255.

Caudal, F., and Glotin, H. (**2008**). "Accuracy analyses of passive tracking of several clicking sperm whales—A case of complex sources binding," in *SIGMAP 2008: Proceedings of the International Conference on Signal Processing and Multimedia Applications*, pp. 55–62.

Congdon, P. (**2003**). *Applied Bayesian Modelling* (Wiley Series in Probability and Statistics) (John Wiley & Sons, Ltd., Chichester, England).

Cranch, G., Crickmore, R., Kirkendall, C., Bautista, A., Daley, K., Motley, S., Salzano, J., Latchem, J., and Nash, P. (**2004**). "Acoustic performance of a large-aperture, seabed, fiber-optic hydrophone array," J. Acoust. Soc. Am. **115**(6), 2848–2858.

Davis, N., and Pitre, R. (**1995**). "Application of probability modeling and Bayesian inversion to passive sonar signal processing. II. Application to ocean acoustic source localization," J. Acoust. Soc. Am. **97**(2), 993–1005.

Dosso, S. E., and Wilmut, M. J. (**2011**). "Bayesian multiple-source localization in an uncertain ocean environment," J. Acoust. Soc. Am. **129**(6), 3577–3589.

Growcott, A., Miller, B., Sirguey, P., Slooten, E., and Dawson, S. (**2011**). "Measuring body length of male sperm whales from their clicks: The relationship between inter-pulse intervals and photogrammetrically measured lengths," J. Acoust. Soc. Am. **130**(1), 568–573.

Hayes, S., and Mellinger, D. (**2000**). "An inexpensive passive acoustic system for recording and localizing wild animal sounds," J. Acoust. Soc. Am. **107**, 3552–3555.

Hirotsu, R., Ura, T., Kojima, J., Sugimatsu, H., Bahl, R., and Yanagisawa, M. (**2008**). "Classification of sperm whale clicks and triangulation for real-time localization with SBL arrays," in *Proceedings of the IEEE Oceans'08*, pp. 553–559.

Hirotsu, R., Yanagisawa, M., Ura, T., Sakata, M., Sugimatsu, H., Kojima, J., and Bahl, R. (**2010**). "Localization of sperm whales in a group using clicks received at two separated short baseline arrays," J. Acoust. Soc. Am. **127**(1), 133–147.

Hooker, S., and Baird, R. (**1999**). "Deep-diving behaviour of the northern bottlenose whale, Hyperoodon ampullatus (Cetacea: Ziphiidae)," Proc. R. Soc. London, Ser. B **266**(1420), 671–676.

Houegnigan, L., Zaugg, S., van der Schaar, M., and Andre, M. (**2010**). "Space-time and hybrid algorithms for the passive acoustic localization of sperm whales and vessels," Appl. Acoust. **71**(11, SI), 1000–1010.

Johnson, M., Aguilar de Soto, N., and Madsen, P. T. (**2009**). "Studying the behaviour and sensory ecology of marine mammals using acoustic recording tags: A review," Mar. Ecol.: Prog. Ser. **395**, 55–73.

Lambert, P., Sutton, A., Burton, P., Abrams, K., and Jones, D. (**2005**). "How vague is vague? A simulation study of the impact of the use of vague prior distributions in MCMC using WinBUGS," Stat. Med. **24**, 2401–2428.

Laplanche, C. (**2007**). "A Bayesian method to estimate the depth and the range of phonating sperm whales using a single hydrophone," J. Acoust. Soc. Am. **121**, 1519–1528.

Laplanche, C., Adam, O., Lopatka, M., and Motsch, J. (**2005**). "Male sperm whale acoustic behavior observed from multipaths at a single hydrophone," J. Acoust. Soc. Am. **118**, 2677–2687.

Laplanche, C., Adam, O., Lopatka, M., and Motsch, J. (**2006**). "Measuring the off-axis angle and the rotational movements of phonating sperm whales using a single hydrophone," J. Acoust. Soc. Am. **119**, 4074–4082.

Madsen, P. T., and Wahlberg, M. (**2007**). "Recording and quantification of ultrasonic echolocation clicks from free-ranging toothed whales," Deep-Sea Res., Part I **54**(8), 1421–1444.

Miller, B., and Dawson, S. (**2009**). "A large-aperture low-cost hydrophone array for tracking whales from small boats," J. Acoust. Soc. Am. **126**(5), 2248–2256.

Miller, P., Johnson, M., Tyack, P., and Terray, E. (**2004**). "Swimming gaits, passive drag and buoyancy of diving sperm whales. Physeter macrocephalus," J. Exp. Biol. **207**, 1953–1967.

Nielsen, B. K., and Mohl, B. (**2006**). "Hull-mounted hydrophones for passive acoustic detection and tracking of sperm whales (*Physeter macrocephalus*)," Appl. Acoust. **67**(11–12, SI), 1175–1186.

Nosal, E.-M., and Frazer, L. N. (**2007**). "Sperm whale three-dimensional track, swim orientation, beam pattern, and click levels observed on bottom-mounted hydrophones," J. Acoust. Soc. Am. **122**(4), 1969–1978.

Ntzoufras, I. (**2009**). *Bayesian Modeling using WinBUGS (Wiley Series in Computational Statistics)* (John Wiley & Sons, Inc., Hoboken, New Jersey).

Robert, C., and Casella, G. (**2010**). *Monte Carlo Statistical Methods*, 2nd ed. (Springer Texts in Statistics) (Springer, New York).

Rowe, D. (**2002**). *Multivariate Bayesian Statistics: Models for Source Separation and Signal Unmixing* (Chapman and Hall/CRC, Boca Raton, Florida).

Sanchez-Garcia, A., Bueno-Crespo, A., and Sancho-Gomez, J. L. (**2010**). "An efficient statistics-based method for the automated detection of sperm whale clicks," Appl. Acoust. **71**(5), 451–459.

Skarsoulis, E., and Kalogerakis, M. (**2005**). "Ray-theoretic localization of an impulsive source in a stratified ocean using two hydrophones," J. Acoust. Soc. Am. **118**(5), 2934–2943.

Spiegelhalter, D., Best, N., Carlin, B., and van der Linde, A. (**2002**). "Bayesian measures of model complexity and fit," J. R. Stat. Soc. Ser. B (Stat. Methodol.) **64**(4), 583–639.

Spiesberger, J. (**2001**). "Hyperbolic location errors due to an insufficient number of receivers," J. Acoust. Soc. Am. **109**, 3076–3079.

Spiesberger, J. (**2005**). "Probability distributions for locations of calling animals, receivers, sound speeds, winds, and data from travel time differences," J. Acoust. Soc. Am. **118**, 1790–1800.

Teloni, V., Johnson, M., Miller, P., and Madsen, P. (**2008**). "Shallow food for deep divers: Dynamic foraging behavior of male sperm whales in a high latitude habitat," J. Exp. Mar. Biol. Ecol. **354**(1), 119–131.

Thode, A. (**2004**). "Tracking sperm whale (*Physeter macrocephalus*) dive profiles using a towed passive acoustic array," J. Acoust. Soc. Am. **116**, 245–253.

Thode, A., Mellinger, D., and Stienessen, S. (**2002**). "Depth-dependent acoustic features of diving sperm whales (*Physeter macrocephalus*) in the Gulf of Mexico," J. Acoust. Soc. Am. **112**, 308–321.

Tiemann, C., Thode, A., Straley, J., O'Connell, V., and Folkert, K. (**2006**). "Three-dimensional localization of sperm whales using a single hydrophone," J. Acoust. Soc. Am. **120**, 2355–2365.

Tollefsen, D., and Dosso, S. E. (**2010**). "Three-dimensional source tracking in an uncertain environment via Bayesian marginalization," J. Acoust. Soc. Am. **128**(3), 111–116.

Wahlberg, M., Møhl, B., and Madsen, P. (**2001**). "Estimating source position accuracy of a large-aperture hydrophone array for bioacoustics," J. Acoust. Soc. Am. **109**, 397–406.

Watwood, S., Miller, P., Johnson, M., Madsen, P., and Tyack, P. (**2006**). "Deep-diving foraging behaviour of sperm whales (*Physeter macrocephalus*)," J. Anim. Ecol. **75**(3), 814–825.

Whitehead, H. (**2003**). *Sperm Whales: Social Evolution in the Ocean* (The University of Chicago Press, Chicago).

Yack, T. M., Barlow, J., Roch, M. A., Klinck, H., Martin, S., Mellinger, D. K., and Gillespie, D. (**2010**). "Comparison of beaked whale detection algorithms," Appl. Acoust. **71**, 1043–1049.